

Complex permittivity of a conductor-loaded dielectric

This article has been downloaded from IOPscience. Please scroll down to see the full text article.

1990 J. Phys.: Condens. Matter 2 4935

(<http://iopscience.iop.org/0953-8984/2/22/014>)

View [the table of contents for this issue](#), or go to the [journal homepage](#) for more

Download details:

IP Address: 171.66.16.103

The article was downloaded on 11/05/2010 at 05:57

Please note that [terms and conditions apply](#).

Complex permittivity of a conductor-loaded dielectric

Perambur S Neelakanta

Department of Electrical Engineering, Florida Atlantic University, Boca Raton, FL
33431, USA

Received 28 September 1989

Abstract. The complex permittivity of a composite dielectric containing conducting inclusions is derived. The shape of the inclusions is described by their aspect ratio. The resultant equations describe the frequency dependence of the permittivity exactly, without recourse to empirically derived parameters.

1. Introduction

Conductor-loaded dielectric materials are useful as radar-absorbing materials, static-dissipative plastics [1], bioelectromagnetic phantoms [2], conducting coatings [3], EMI shields [4], conductive adhesives [5], etc. Typical inclusions like flaky graphite lamellae, needle-like metallic fibres or near-spherical conducting powders can be used to alter the dielectric and conductivity characteristics of an insulating host medium significantly. The effective permittivity and/or conductivity of the mixture are decided by: (i) volume fraction, geometrical shape and conductivity of the inclusions; and (ii) electric susceptibility of the host dielectric. Two other deciding factors are the frequency and statistical aspects of the random particulate dispersion in the mixture.

Existing formulations [3, 6–43], which describe the dielectric behaviour of heterogeneous systems, in general, refer to: (1) calculation of effective permittivity of the mixtures; and (ii) calculation of dielectric loss associated with such heterogeneous systems. Most often, as indicated by van Beek [6], development of mixture-permittivity formulations and analyses of dielectric loss phenomena have been treated as two independent strategies.

Confining attention to binary mixtures of homogeneous, isotropic non-conducting constituents (pure dielectric–dielectric mixtures), the calculation of relative permittivity of the mixture has received considerable attention [6, 7]; the mixture permittivity is expressed in terms of the permittivities and volume fractions of the constituents. In the absence of an explicit parameter depicting the shape of the constituent particulates, most of the mixture formulations are quasi-empirical in nature, and the reliability of their applicability to random binary mixtures has been regarded as questionable [7]. However, for well defined geometries (such as spheres, ellipsoids, etc), application of electrostatic potential theory and polarisation considerations has enabled near-exact formulations as described by Calderwood and Scaife [7] and by Fricke [8, 9].

In the evaluation of relative permittivity of dielectric–dielectric mixtures, the components of the heterogeneous systems have been tacitly assumed to be loss-free [6], but

this conditions is not often fulfilled. The loss phenomena associated with dielectric mixtures are due to the various polarisations caused by relative displacement of electrons and nuclei, dipolar orientations and interfacial (Maxwell–Wagner) effects [10] at the boundaries between the mixture components [6]. The lossy behaviour of the mixture becomes even more pronounced when a conducting material (such as metallic particles, graphite lamellae, etc) is dispersed as a constituent in a dielectric–conductor mixture [11–21].

Inasmuch as dielectric loss is a polarisation-based phenomenon, it is frequency-dependent due to relaxation effects and is strongly influenced by the particulate geometry. In other words, a heterogeneous mixture with conducting inclusions should be characterised by complex permittivity parameters depicting the dielectric spectrum and its explicit dependence on particle geometry (apart from the volume fractions, permittivities and conductivities of the mixture components). Ideally, the complex permittivity spectra, namely the variations of relative permittivity and conductivity (or dielectric loss) of the conductor-loaded mixture with frequency, should be tractable by non-empirical formulations. All the included parameters of such formulations should be explicit quantities derived from the input values of permittivities, and conductivities and particulate geometry of the mixture constituents.

For conducting inclusions of simple shape (such as spheres, spheroids, etc) dispersed randomly in a host medium, and for existing formulations such as those of Fricke [8, 9] or those described in [6], the geometrical aspect of the particulates has been accommodated as a shape factor. But, the frequency dependence of the relative permittivity has been specified only as limiting values, namely, ϵ_s (static permittivity) and ϵ_∞ (permittivity at infinitely high frequency), as per Debye's complex admittance relation [6]. The frequency dependence of the permittivity characteristics of a lossy mixture dielectric, however, has not been explicitly formulated; a semiempirical approach based on frequency-independent limiting values of relative permittivity (such as those given by equations (3.27), (3.28), (3.38) and (3.39) in [6]) is often resorted to in the description of dielectric spectra. Specific to mixtures constituted by shaped inclusions randomly dispersed in a host dielectric (with a significant volume fraction), the dielectric spectral formulations that have been adopted are therefore purely empirical; and they are decided largely by curve-fitting strategies on experimental data [12–14].

In the present study, however, an analytical method is proposed to derive non-empirical, closed-form solutions to describe the relative permittivity and conductivity spectra of a conductor-loaded dielectric. This is done by extending the logarithmic law of mixing [22–27] to complex dielectric susceptibility and choosing an appropriate order function to depict the influence of particulate geometry on dielectric polarisation. In addition, the following are also taken into consideration. (i) The host receptacle (dielectric) and the inclusions (conductor) are electrically non-conducting and conducting, respectively. (ii) Such extreme characterisations of the mixture components render the test mixture either conductivity-dominant or permittivity-dominant, depending on whether the ratio $\sigma/\omega\epsilon_0\epsilon$ is large or small; here σ and ϵ refer to the conductivity and relative permittivity of the mixture respectively, ω is the angular frequency and ϵ_0 is the free-space permittivity. (iii) Depending on the volume fraction of conductor loading, random current paths could also be formed, which may cause an erratic transitory switching from a low- to a high-conductivity property of the mixture [19].

Earliest versions of conductor–dielectric mixture formulations are due to Maxwell [28] and Rayleigh [29], who, on the basis of classical Clausius–Mosotti/Lorentz–Lorenz concepts of electrostatics, derived the static permittivity of a dielectric dispersed with a

dilute phase of conducting inclusions. Bruggeman [30] extended Rayleigh's formula by considering incremental changes in volume loading and arrived at the so-called 1/3 power law. Replacing the 1/3 exponent with an empirical constant, the relevant formulation has become known as Archie's law [31].

In more rigorous and recent analyses, two types of approach as indicated earlier have been pursued. In the first method, the dielectric effects and conductive effects are treated independently [11–13, 30, 31]. The other method considers the effect of the conductor as a loss factor, with the assumption of a conductor having infinite permittivity [14–16, 20, 32]. In both approaches, however, only the static (DC) values have been evaluated.

Thus, Lal and Parshad [14] extended the pure dielectric–dielectric mixture theory to a dielectric–conductor composite, and derived an expression for the static (relative) permittivity of the mixture (ϵ_s) in terms of the volume ratio θ of the conductor inclusions:

$$\epsilon_s = \epsilon_{2s}/(1 - \theta)^B. \quad (1)$$

In this relation, ϵ_{2s} is the static permittivity of the host dielectric and B is a shape parameter of the conducting particles, related to the depolarisation factors A_i via

$$B = \frac{1}{3} \sum_i A_i. \quad (2)$$

The subscript i refers to the i th axis of an ellipsoid with axes a , b and c . For a spheroidal particle $b = c$ and, defining $x = a/b$, $x = 1$ specifies spherical particles. Prolate spheroidal particles with $x > 1$ will become needle-like fibres when $x \gg 1$. Likewise, oblate spheroids with $x < 1$ will represent flaky, disc-like lamellae when $x \ll 1$. A_i can be evaluated by an integral relation due to Wallin [17].

It may be noted that equation (1) cannot be extended to frequency-dependent dynamic conditions; nor is evaluation of B straightforward. Results presented in [14] are therefore based on an empirical value of B obtained via curve fitting to a set of test data.

Considering the conductivity of the test mixture, Scarisbrick [12] developed a random-chain model, to which Kusy [13] added a shape-dependent order function (U) established via probabilistic considerations. Again, the relevant expression refers only to DC conductivity of the mixture and is given by

$$\sigma_{DC} = K^2 \sigma_1 \theta^{1+U\theta^{-2/3}} \quad (3)$$

where K is a constant decided by the conductive path cross section and U is an order function.

Frame and Tedford [3] used equations (1) and (3) to evaluate the static permittivity and DC conductivity of a composite made of alkyd resin loaded with graphite lamellae. In the relevant studies, the exponent B of equation (1) best-fitted to experimental data on static permittivity was 6.2. The corresponding calculated value, $A = 1/13$, was then compared against the average geometrical aspect ratio. In other words, absolute determination of ϵ_s via equation (1) is not straightforward even with an *a priori* knowledge of particulate geometry.

Further, though Frame and Tedford [3] measured the dielectric spectrum of the test mixture, their results could not be compared with any theoretical results due to the lack of availability of any relevant frequency-dependent formulation.

Considering the mixture conductivity, equation (3) could be best-fitted to the experimental data of Frame and Tedford [3] only with an unjustifiable presumption of the resistivity of graphite being $1 \Omega\text{m}$ (which is far greater than the established value of

$5 \times 10^{-3} \Omega\text{m}$). Moreover, the 'best-fitted' curve hardly matches the experimental data at high and low volume fractions of inclusions (see figure 4 of [3]). Thus, even the rigorous formulation based on the model of Scarisbrick [12] and Kusy [13] seems to be semiempirical.

In view of the aforesaid shortcomings and persisting incompatibility of the existing formulations, it is attempted here to develop a dielectric-conductor mixture model based on complex susceptibility considerations.

2. Complex susceptibility model

Let ε and σ denote the relative permittivity and conductivity of the mixture. Subscripts 1 and 2 are used to specify the corresponding variable of the conducting inclusions and the dielectric matrix, respectively. The volume fraction of the inclusions is denoted by θ , and U is an order function decided by the geometrical aspect ratio ($x = a/b$) of the inclusions.

The electrical characteristics of a mixture formed by a random volumetric dispersion of shaped inclusions in a continuous host medium can be specified by functional relations

$$f(\varepsilon) = \theta f(\varepsilon_1) + (1 - \theta)f(\varepsilon_2)$$

and

$$g(\sigma) = \theta g(\sigma_1) + (1 - \theta)g(\sigma_2).$$

Here, the functions f and g determine the law of mixing and, if they are known explicitly, the values of ε and σ can be determined uniquely. The law of mixing pertaining to a statistical mixture is constrained by: (i) Wiener's proportionality postulate [33, 34]; (ii) Wiener's upper and lower bounds on ε and σ ; (iii) the limiting values of $0 \leq \theta \leq 1$ and $0 \leq U \leq 1$; and (iv) geometrical dissimilarity of the components in the mixture matrix.

The analytical endeavour of evaluating the functions f and/or g for various types of pure dielectric-dielectric mixtures resulted in several formulations; a comprehensive review of them has been published by Brown [35] and van Beek [6]. The contents of these reviews have also been summarized and reported by Tinga and Voss [36].

These formulations, however, ignore the chaotic aspects of the mixture, except the so-called logarithmic law of mixing due to Lichtenecker [26, 27]. But this logarithmic law, however, does not take the particulate geometry into account, as well as lacking a linear form [23, 37]. These deficiencies have, however, been offset by the author and others as reported in [22, 23].

In the following analysis, the logarithmic law is extended to a generalised electric susceptibility parameter χ pertaining to a dielectric plus conductor mixture subjected to complex field [38] considerations. Hence, a dynamic model is developed to calculate the effective complex permittivity of the test mixture.

The complex susceptibility of a conductor-loaded mixture can be specified as a logarithmic model in the following form:

$$\log \chi = \theta \log \chi_1 + (1 - \theta) \log \chi_2. \quad (4)$$

In terms of the explicit parameters of the mixture constituents, namely $(\varepsilon_1, \sigma_1)$ and $(\varepsilon_2, \sigma_2)$, equation (4) can be written as

$$\chi = (\sigma_1/\omega\varepsilon)^\theta \exp(i\pi\theta/2) \{[(\varepsilon_2 - 1)^2 + (\varepsilon_2 \tan \delta_2)^2]^{1/2} \exp(-i\varphi)\}^{1-\theta} \quad (5)$$

where ε_0 is the free-space permittivity, $\omega = 2\pi \times$ frequency, $\tan \delta_2 (= \sigma_2/\omega\varepsilon_0\varepsilon_2)$ is the loss tangent of the host medium and $\varphi = \tan^{-1}[\varepsilon_2 \tan \delta_2/(\varepsilon_2 - 1)]$.

Using the relation $(\epsilon - 1) = \text{Re } \chi$, it follows that

$$\epsilon = (\sigma_1/\omega\epsilon_0)^\theta [(\epsilon_2 - 1)^2 + (\epsilon_2 \tan \delta_2)^2]^{(1-\theta)/2} \cos[\pi\theta/2 + \varphi(1 - \theta)] + 1. \tag{6}$$

The conductivity (σ) of the mixture can be extracted from $\text{Im } \chi$. Thus,

$$\sigma/\omega\epsilon_0 = (\sigma_1/\omega\epsilon_0)^\theta [(\epsilon_2 - 1)^2 + (\epsilon_2 \tan \delta_2)^2]^{(1-\theta)/2} \sin[\pi\theta/2 + \varphi(1 - \theta)] + 1. \tag{7}$$

Equations (6) and (7) should, however, be ‘weighted’ to meet the limiting conditions, namely $(\epsilon, \sigma) = (\epsilon_2, \sigma_2)$ at $\theta = 0$ and (ϵ_1, σ_1) at $\theta = 1$.

Further, by including the geometrical dependence via an order function U in the logarithmic formulation of equation (4), the following modified expressions for ϵ and σ are obtained on the basis of the arguments given by the author elsewhere [23]:

$$\epsilon_{\text{mod}} = C_1 [(\epsilon - 1)^{U_\epsilon} + 1] \tag{8}$$

and

$$\sigma_{\text{mod}}/\omega\epsilon_0 = C_2 [(\sigma_1/\omega\epsilon_0)^\theta (\epsilon_2 - 1)^{1-\theta} \sin(\pi\theta/2)]^{U_\sigma} + (\sigma_2/\omega\epsilon_0) \tag{9}$$

under the valid assumptions that $\sigma_2 \ll \sigma_1$ and $\epsilon_2 \tan \delta_2 \ll (\epsilon_2 - 1)$. Here, the coefficients C_1 and C_2 are weighting coefficients decided by the limiting conditions, namely $\epsilon = \epsilon_2$ at $\theta = 0$ and $\sigma = \sigma_1$ at $\theta = 1$. Hence, they are specified explicitly as

$$C_1 = \epsilon_2 [(\epsilon_2 - 1)^{U_\epsilon} + 1]^{-1} \tag{10a}$$

and

$$C_2 = [(\sigma_1 - \sigma_2)/\omega\epsilon_0] (\omega\epsilon_0/\sigma_1)^{U_\sigma}. \tag{10b}$$

The order functions U_ϵ and U_σ implicitly determine the dependence of ϵ and σ , respectively, on the geometrical aspect ratio $x (=a/b)$ of the particulate inclusion. Defining the particle eccentricity $e (=1 - b/a)$ when $b < a$ or $(a/b - 1)$ when $a < b$, the value of $e = 0$ corresponds to spherical particles; U_ϵ and U_σ should therefore be expressed in terms of e . That is, for a given eccentricity, the U_ϵ th fraction of the chaotic system can be regarded as being polarised along the electric field and the $(1 - U_\epsilon)$ th fraction along the orthogonal direction. Likewise, U_σ should represent the fraction corresponding to current percolations.

On the basis of similarity to Maxwell–Boltzmann statistics applied to dipole orientation [39], the upper and lower bounds of the order function can be specified as follows:

$$U_U = \frac{1}{2}[1 - L(e)/e] \quad \approx 1/3 \quad \text{when } e \rightarrow 0 \tag{11a}$$

$$U_L = \frac{1}{2}[L(e)/e] \quad \approx 1/6 \quad \text{when } e \rightarrow 0 \tag{11b}$$

where $L(e)$ is the Langevin function, equal to $\coth(e) - 1/e$. The functions U_ϵ and U_σ can be equated to U_L or U_U depending on the following states of the test mixture. For large values of $(\sigma_1/\omega\epsilon_0\epsilon_2)$, the composite can be considered as conductivity-dominant; and, for low values of $(\sigma_1/\omega\epsilon_0\epsilon_2)$, the mixture becomes permittivity-dominant. Accordingly, the permittivity of the mixture as a function of frequency can be sketched as shown

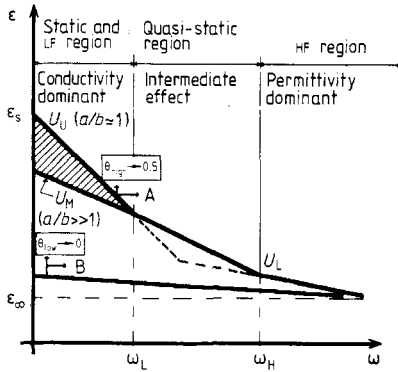


Figure 1. Permittivity versus frequency of a conductor-loaded dielectric: curve A, for large volume fractions θ of inclusions; curve B, for low volume fractions θ of inclusions. The shaded region refers to the bounded range of values that ϵ may assume as decided by the aspect ratio of conducting inclusions ($1 \leq a/b \leq \infty$).

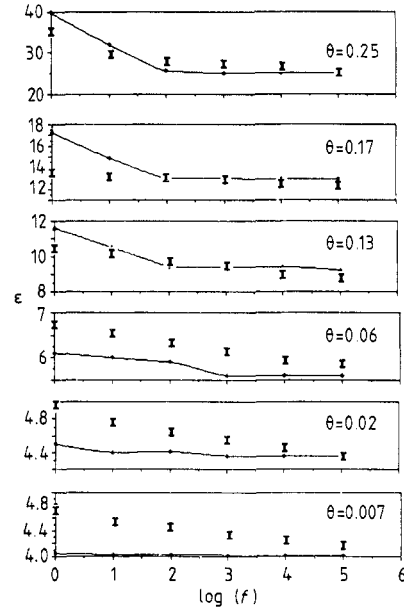


Figure 2. Dielectric spectrum of alkyd resin plus graphite. The bold 'error bars' (I) show experimental data [3]. The small points (◆) and full curves show theoretical results of present method.

in figure 1, indicating three zones, namely, the low-frequency, the high-frequency and the intermediate (quasi-static) regions. It is, however, to be noted that the region-to-region transition is not abrupt. For calculation purposes, two corner frequencies, namely ω_L and ω_H , can be approximately assigned marking the transitions as shown in figure 1, since the regions are distinguishable in terms of $d\epsilon'/d\omega$ slope. In summary, the complex permittivity spectra of a conductor-loaded mixture can be specified by the following:

(i) Complex permittivity of the mixture (ϵ)

$$\epsilon = \epsilon' - i\epsilon'' \tag{12a}$$

$$\epsilon' = \{\epsilon_2/[1 + (\epsilon_2 - 1)U_\epsilon]\} \{[(\sigma_1/\omega\epsilon_0)^\theta (\epsilon_2 - 1)^{1-\theta} \cos(\pi\theta/2)U_\epsilon + 1]\} \tag{12b}$$

$$\epsilon'' = \sigma/\omega\epsilon_0\epsilon' \tag{12c}$$

$$\sigma = (\sigma_1 - \sigma_2) \{[\omega\epsilon_0(\epsilon_2 - 1)/\sigma_1]^{1-\theta} \sin(\pi\theta/2)\}^{u_\sigma} + \sigma_2. \tag{12d}$$

(ii) Order functions U_ϵ and U_σ at low frequencies ($\omega < \omega_L$)

$$U_\epsilon = U_\sigma = \begin{cases} U_U = \frac{1}{2}[1 - L(e)/e] & e = 0 \\ U_M = (1/M) + (2 - 3M)/3 & e \gg 1 \end{cases} \tag{13a}$$

$$\tag{13b}$$

where $M = [(2 \pm e)/(3 \pm e) - L'(e)]^{-1}$ and $L'(e) = dL/de$; the positive sign here refers to $a/b < 1$ and the negative sign is for $a/b > 1$.

(iii) Order functions U_ϵ and U_σ at high frequencies ($\omega > \omega_H$)

$$U_\epsilon = U_\sigma = U_L = \frac{1}{2}[L(e)/e] \quad \text{for all values of } e. \quad (14)$$

(iv) Calculation of approximate values of ω_L and ω_H (figure 1)

$$\omega_H \text{ is the solution of } \quad \epsilon_{\text{mod}}(\text{with } U_L) \approx \epsilon_{\text{mod}}(\text{with } U_U) \quad (15a)$$

and

$$\omega_L \text{ is the solution of } \quad \epsilon_{\text{mod}}(\text{with } U_L) \approx \epsilon_{\text{mod}}(\text{with } U_M). \quad (15b)$$

(v) Complex permittivity in the quasi-static range ($\omega_L < \omega < \omega_H$)

$$\epsilon' = \epsilon'_L - (\epsilon'_L - \epsilon'_H)[\ln(\omega/\omega_L)]/[\ln(\omega_H/\omega_L)] \quad (16a)$$

$$\epsilon'' = \sigma/\omega\epsilon_0\epsilon' \quad (16b)$$

$$\sigma = \sigma_L - (\sigma_L - \sigma_H)[\ln(\omega/\omega_L)]/[\ln(\omega_H/\omega_L)] \quad (16c)$$

where (ϵ'_L, σ_L) and (ϵ'_H, σ_H) refer to values of (ϵ', σ) at ω_L and ω_H , respectively.

3. Direct-current conductivity

Equation (9) can be rewritten to represent the static conductivity (σ_{DC}) of the mixture. The DC condition refers to the limiting case of $\omega \rightarrow 0$, or a factor τ_0 (which is extremely large) should replace $\omega/2\pi$ in equation (9). The factor τ_0 can be evaluated under the condition $x \rightarrow 1, \theta \rightarrow \frac{1}{2}, U_\sigma \rightarrow 1$ and $\sigma_{\text{DC}} \approx (\sigma_1\sigma_2)^{1/2}$, representing the weighted-average value. It is found that

$$\sigma_{\text{DC}} \approx (\sigma_1 - \sigma_2) \{ [2\pi\epsilon_0(\epsilon_2 - 1)/\sigma_1\tau_0]^{1-\theta} \sin(\pi\theta/2) \}^{U_\sigma} + \sigma_2 \quad (17a)$$

with

$$\tau_0 = \frac{\pi\epsilon_0(\epsilon_2 - 1)}{\sigma_2} \frac{\sigma_1^{1/2} + \sigma_2^{1/2}}{\sigma_1^{1/2} - \sigma_2^{1/2}} \quad (17b)$$

and

$$U_\sigma = U_U = \frac{1}{2}[1 - L(e)/e]. \quad (17c)$$

4. Results and discussion

4.1. Dielectric permittivity of the text mixture

To verify the present formulations, results on the permittivity pertaining to a few dielectric-conductor mixtures, for which experimental data are available, were

computed. The results are given in table 1. Further, the theoretical results due to the present method on the permittivity of a typical dispersed system, as a function of frequency, are presented in table 2, along with the measured/calculated data due to Frame and Tedford [3]. On the basis of these results, the following inferences are made.

The method of Lal and Parshad [14] requires the determination of shape factor (denoted as B in [14]), either via an involved calculation of depolarisation factor (in terms of a/b) or by experiments. Comparable results can, however, be obtained with ease by the present closed-form relation of equation (12).

Referring to table 1, the aspect ratios (a/b) used in the present formulation, namely 1/13, 1 and 1.3, closely correspond to the respective values of 1/13 (graphite lamellae), 1 (mercury globules) and 1 (near-spherical iron particles) adopted in the best-fit experimental data.

Considering the data on epoxy plus aluminium particles [14], the present method yields results close to measured values, assuming $a/b = 1.5$. This corresponds to the particle inclusions being non-spherical, concurring with the experimental observation that the particles were spheroidal.

The logarithmic-law-based calculation in [16] (without the particle shape being considered) could be best-fitted to experimental data only with an unjustifiable assumption of the permittivity of the metal (aluminium) being 165. Thus, whereas the results of [16] are totally empirical, the present analysis is free from this deficiency.

4.2. Dielectric spectrum

Inasmuch as the formulation of Lal and Parshad [14] involves no frequency parameter, the dielectric spectrum of alkyd plus graphite mixture measured by Frame and Tedford [3] was not compared with any theoretical results in [3]. The present formulation (equation (12)), however, has the explicit ω term to characterise the dynamic response of the test mixture. Hence, computed results based on equation (12) are depicted in figure 2 (and in table 2) along with the measured data due to Frame and Tedford [3]. As discussed earlier, two approximate corner frequencies $\omega_L (= 2\pi \times 10^3)$ and $\omega_H (= 2\pi \times 10^6)$ were calculated (equation (17)) and used in the calculations. Close agreement between theory and experiment is evident; again, it should be noted that the theoretical results are totally free from any empirical parameters.

4.3. DC conductivity data

Measured data on the resistivity of alkyd plus graphite mixture obtained from Frame and Tedford [3] are presented in figure 3 along with the best-fit curve (curve A) based on Scarisbrick [12] and Kusy [13] formulations. Curve A was best-fitted [14] assuming the resistivity of graphite as $1 \Omega\text{m}$, which is much different from the established value of $5 \times 10^{-3} \Omega\text{m}$. Thus, curve A can be regarded only as an empirical result.

Shown in figure 3 is also a curve obtained by the present method (equation (17a)) with the data available in [14], namely, graphite conductivity = 200 S (corresponding to $\rho_1 = 5 \times 10^{-3} \Omega\text{m}$) and a/b ratio of the particles equal to 1/13. Since conductivity effects dominate at DC, U_σ was set equal to U_U and τ_0 was decided by equation (17b).

In figure 4 measured data on the DC conductivity of a mixture of bakelite plus silver particles (due to Garland [43]) are presented along with the theoretical results obtained by the present method.

Table 1. Measured and computed data: permittivity of dielectric-conductor mixture.

| Mixture | | Volume fraction of inclusions, θ | | | Calculated data on ϵ | | | Measured data on ϵ | | |
|---|--|---|-----------------------------|--|--------------------------------------|---------|----------------|-----------------------------|----------------|---|
| Host dielectric medium (ϵ_2) | Conducting inclusions (σ) | Frequency (Hz) | Present method | Other method(s) | | Remarks | ϵ | Remarks | ϵ | Remarks |
| | | | | Semiempirical best-fit data (ϵ) | Remarks | | | | | |
| Alkyd resin (3.86) | Graphite lamellae (200 S m^{-1}) Aspect ratio $a/b \ll 1$ | 10^3 | $a/b = 1/13$ $U_i = U_M$ | 4.01 | $b/a = 13$ | | 4.01 \pm 6% | | 4.01 \pm 6% | [3] |
| | | | | 4.37 | Shape factor | | 4.37 \pm 6% | | 4.37 \pm 6% | |
| | | | | 5.66 | $B = 6.2$ | | 5.66 \pm 6% | | 5.66 \pm 6% | |
| | | | | 9.15 | [3] | | 9.15 \pm 6% | | 9.15 \pm 6% | |
| | | | | 12.25 | | | 12.25 \pm 6% | | 12.25 \pm 6% | |
| Epoxy (3.81) | Aluminium needles ($3.77 \times 10^7 \text{ S m}^{-1}$) $a/b > 1$ | 1.6×10^6 | $B = 4.42$ | 4.59 | Logarithmic model [16] | | 4.71 | | 4.71 | [16] |
| | | | | 5.55 | | | 5.60 | | 5.60 | |
| | | | | 6.70 | $\epsilon_1 = 165$ | | 7.10 | | 7.10 | |
| | | | | 8.09 | Empirical | | 8.18 | | 8.18 | |
| | | | | 9.77 | value unjustifiably presumed in [16] | | 9.16 | | 9.16 | |
| 11.80 | $\epsilon_2 = 3.81$ | | 12.05 | | 12.05 | | | | | |
| Aetna oil (2.21) | Mercury drops (10^6 S m^{-1}) $a/b \approx 1$ | 10^3 | $a/b = 1$ $U_i = U_L$ | 2.31 | $a/b = 1$ | | 2.31 | | 2.31 | Data due to Guillein as reported in [14] |
| | | | | 2.57 | Shape factor | | 2.57 | | 2.57 | |
| | | | | 3.88 | $B = 3$ | | 3.94 | | 3.94 | |
| | | | | 5.24 | [14] | | 5.34 | | 5.34 | |
| | | | | 7.30 | (Bruggeman's formula) | | 7.15 | | 7.15 | |
| 10.27 | | | 9.67 | | 9.67 | | | | | |
| Mineral oil (2.1) | Iron spheroidal particles (10^7 S m^{-1}) $a/b > 1$ | 10^3 | $a/b = 1.3$ $U_i = U_L$ | 2.60 | $a/b > 1$ | | 2.60 | | 2.60 | Data due to Nasuhoglu as reported in [14] |
| | | | | 3.30 | Shape factor | | 3.30 | | 3.30 | |
| | | | | 3.57 | $B \approx 3.96$ | | 4.00 | | 4.00 | |
| | | | | 4.47 | [14] | | 4.90 | | 4.90 | |
| | | | | 5.56 | (Bruggeman's formula) | | 6.25 | | 6.25 | |

Table 2. Measured and computed data: dynamic response of dielectric-conductor mixture.

| Host dielectric medium (ϵ_2) | Mixture | Conducting inclusions (σ) | Frequency (Hz) | Calculated and measured data on mixture permittivity (ϵ) | | | | | | | | | | U_M | | | |
|---|--|------------------------------------|----------------|---|-----------------|------------------|------|------------------|------|------------------|-------|------------------|-------|-------|------------------|-------|--|
| | | | | $\theta = 0.007^a$ | | $\theta = 0.020$ | | $\theta = 0.060$ | | $\theta = 0.130$ | | $\theta = 0.170$ | | | $\theta = 0.250$ | | |
| | | | | I ^b | II ^c | I | II | I | II | I | II | I | II | I | II | | |
| Alkyd resin (3.86) | Graphite lamellae (200 S m^{-1}) | | 10^1 | 4.60 | 4.03 | 4.80 | 4.40 | 6.60 | 5.87 | 10.00 | 10.46 | 13.20 | 14.98 | 28.60 | 31.86 | | |
| | | | 10^2 | 4.50 | 4.02 | 4.70 | 4.35 | 6.40 | 5.63 | 9.70 | 9.44 | 13.00 | 13.00 | 27.70 | 25.55 | | |
| | Aspect ratio $a/b \ll 1$ | In present calculations | 10^3 | 4.40 | 4.02 | 4.60 | 4.34 | 6.20 | 5.63 | 9.40 | 9.39 | 12.80 | 12.87 | 26.80 | 25.09 | | |
| | | | 10^4 | 4.30 | 4.00 | 4.50 | 4.30 | 6.00 | 5.60 | 9.10 | 9.30 | 12.50 | 12.80 | 25.40 | 25.00 | | |
| | | | 10^5 | 4.10 | 4.00 | 4.40 | 4.30 | 5.90 | 5.60 | 8.70 | 9.30 | 12.00 | 12.80 | 25.00 | 25.00 | | |
| | | | | | | | | | | | | | | | | U_L | |
| | | | | | | | | | | | | | | | | | |

^a Volume fraction of the inclusions: θ .^b Experimental results due to Frame and Tedford [3]: I.^c Calculated data as per the present method: II.

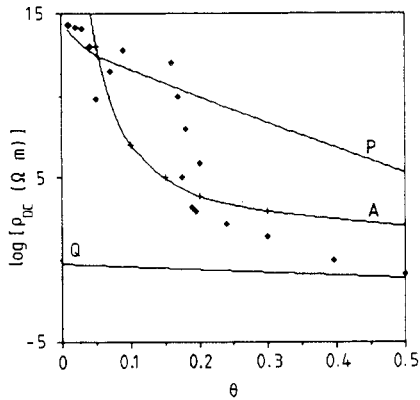


Figure 3. DC resistivity of alkyd resin plus graphite mixture. The diagram shows the theoretical results of the present method (equation (17)) with $U_o = U_U$ (curve P) and with $U_o = U_L$ (curve Q). Data: $\epsilon_2 = 3.86$, $\sigma_1 = 200 \text{ S m}^{-1}$, $a/b = 1/13$, $\rho_2 = 10^{14} \text{ } \Omega\text{m}$ and $\tau_0 = 1/(1.62 \times 10^{-22})$. Also shown are experimental results [3] (\blacklozenge) and best-fit curve ($-+-$) by Scarisbrick [12] and Kusy [13] formulation(s) (curve A).

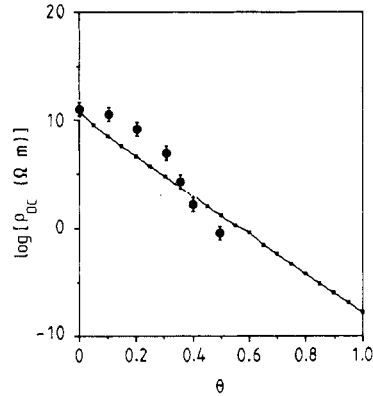


Figure 4. DC resistivity of bakelite plus silver mixture. Data: $\epsilon_2 = 5$, $a/b = 1$, $\sigma_1 = 6.17 \times 10^7 \text{ S m}^{-1}$, $\rho_2 = 10^{11} \text{ } \Omega\text{m}$ and $\tau_0 = 1/(6.8 \times 10^{-37})$. The diagram shows experimental results [43] (\bullet) and theoretical results of present method (equation (17)) with $U_o = U_U$ ($-\blacksquare-$).

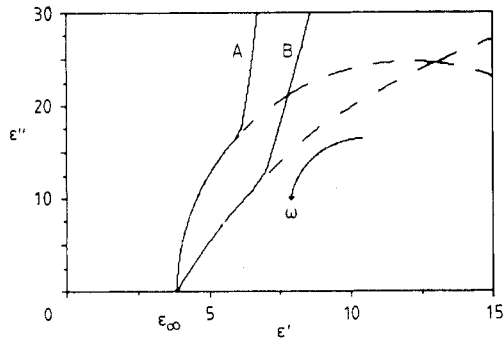


Figure 5. Cole-Cole plot(s) for the alkyd resin plus graphite mixture. Data as in [3]. Curve A, $\theta = 0.17$; curve B, $\theta = 0.25$.

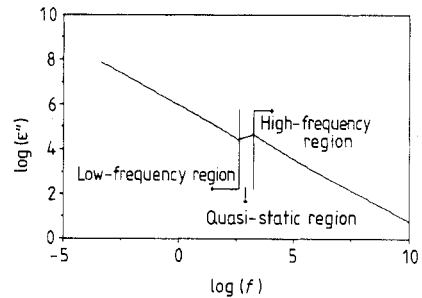


Figure 6. Plot of $\log(\epsilon'')$ versus $\log(f)$ for the alkyd plus graphite mixture. Data as in [3] with volume fraction of graphite $\theta = 0.17$.

In both mixtures (figures 3 and 4), it may be observed that the present theoretical results follow the measured data closely at low and high volume fractions and follow approximately the trend of resistivity transition at the threshold volume fraction.

4.4. Complex permittivity and Cole-Cole diagram

Relevant to the dielectric data on alkyd plus graphite mixture, the calculated ϵ' and ϵ'' as per equation (12c) are depicted by the Cole-Cole diagram in figure-5. The larger

the conductivity of the inclusions, the further the Cole–Cole plot departs from the semicircular diagram.

An alternative graphical representation of plotting the logarithm of ε'' (as per equation (12c)) against the logarithm of ω permits the determination of approximate zoning of conductivity-dominant, permittivity-dominant and quasi-static regions discussed before. Calculated results on alkyd plus graphite mixture are presented in figure 6 for relevant illustration.

4.5. Order functions

Lastly, it may be observed that the order functions in the present studies concerning dielectric–conductor mixtures were evaluated via the Langevin function, which permits compatible limiting conditions, namely, $0 \leq (U_L \text{ or } U_U) \leq 1$ for $0 \leq \theta \leq 1$ of dielectric plus conductor mixtures. For pure dielectric–dielectric mixtures, however, the order functions are decided by a different formulation suggested by Sillars [44], as indicated in [23].

5. Conclusions

A comprehensive approach to evaluate the complex permittivity of a dielectric–conductor mixture is presented. Present studies provide closed-form solutions to evaluate ε' and ε'' of the test mixture, which have been compared with available experimental and empirical formulations.

The complex permittivity expressions have been extended to calculate the DC conductivity (or resistivity) of the mixture and the effects of volume loading of conductive inclusions are studied.

Computed results of the present method closely agree with a number of available data (without resorting to any empirical parameters), indicating the efficacy of the formulations in the practical design of test composites.

References

- [1] Neelakanta P S 1989 *Electron. Packag. Product.* **29** 64
- [2] Hartsgrove G, Krasewsky A and Surowiec A 1987 *Bioelectromagnetism* **8** 29
- [3] Frame R I and Tedford D J 1986 *IEEE Trans. Electr. Insul.* **EI-21** 23
- [4] Davenport D E 1981 *Polym.-Plast. Technol. Eng.* **17** 211
- [5] Nieberlein V N 1976 *IEEE Trans. Compos. Hybrids Manuf. Tech.* **CHMT-1** 172
- [6] van Beek L K H 1967 *Progress in Dielectrics* vol 7, ed J B Birks (London: Iliffe)
- [7] Calderwood J H and Scaife B K P 1979 *IEE Conf. on Dielectric Materials, Measurements and Applications (1979)* (London: IEE Publications)
- [8] Fricke H 1924 *Phys. Rev.* **24** 575
- [9] Fricke H 1926 *Phys. Rev.* **26** 678
- [10] Hamon B V 1953 *Aust. J. Phys.* **6** 304
- [11] Dukhin S S and Shilov V N 1974 *Dielectric Phenomena and the Double-Layer in Disperse Systems and Polyelectrolytes* (New York: Wiley)
- [12] Scarisbrick R M 1973 *J. Phys. D: Appl. Phys.* **6** 2095
- [13] Kusy A 1977 *Thin Solid Films* **43** 243
- [14] Lal K and Parshad R 1973 *J. Phys. D: Appl. Phys.* **6** 1788
- [15] Neelakantaswamy P S and Kisdnasamy S 1984 *Proc. Int. AMSE Conf. (Athens, 1984)* 2.1 (Tassin-lademi-lune: AMSE) p 69

- [16] Paipetis S A, Tsangaris G M and Tsangaris J M 1983 *Polym. Commun.* **24** 373
- [17] Wallin S R 1985 *PhD Thesis* University of Wyoming
- [18] St Onge H 1980 *IEEE Trans. Electr. Insul.* **EI-15** 350
- [19] deAraujo F F T and Rosenberg H M 1976 *J. Phys. D: Appl. Phys.* **9** 1025
- [20] Peyrelasse J, Boned C, Canadas G and Royer R 1984 *Phys. Rev. A* **30** 994
- [21] Rothwell W S 1971 *IEEE Trans. Microwave Theory Tech.* **MTT-19** 413
- [22] Kisdnasamy S and Neelakantaswamy P S 1984 *Electron. Lett.* **20** 291
- [23] Neelakantaswamy P S, Turkman R I and Sarkar T K 1985 *Electron. Lett.* **21** 270
- [24] Neelakantaswamy P S, Chowdary B V R and Rajaratnam R 1983 *J. Phys. D: Appl. Phys.* **17** 1755
- [25] Neelakantaswamy P S, Aspar K and Rajaratnam A 1983 *Biomed. Technik* **28** 18
- [26] Lichtenecker K 1929 *Phys. Z.* **30** 805
- [27] Lichtenecker K and Rother K 1931 *Phys. Z.* **32** 255
- [28] Maxwell J C 1954 *A Treatise on Electricity and Magnetism* vols I and II (New York: Dover)
- [29] Lord Rayleigh 1892 *Phil. Mag.* **34** 481
- [30] Bruggeman D A G 1935 *Ann. Phys., Lpz.* **24** 636
- [31] Archie G E 1942 *Trans. AIME* **146** 54
- [32] Vinogradov A P, Karimov V A M, Kunavin A T, Lagarkov A V, Sarychev A K and Stember N A 1984 *Dokl. Akad. Nauk SSSR* **275** 590
- [33] Wiener O 1912 *Abh. Lpz. Akad.* **32** 509
- [34] Bergman D J 1981 *Phys. Rev. B* **23** 3058
- [35] Brown W F 1956 *Dielectrics in Encyclopedia of Physics* vol 47 (Berlin: Springer)
- [36] Tinga W R and Voss W A G 1973 *J. Appl. Phys.* **44** 3897
- [37] Reynolds J A and Hough J M 1957 *Proc. Phys. Soc.* **70** 769
- [38] Takashima T, Nakae T and Ishibashi R 1980 *IEEE Trans. Electr. Insul.* **15** 1
- [39] Coelho R 1979 *Physics of Dielectrics for the Engineer* (New York: Elsevier) p 27
- [40] Bergman D J 1980 *Phys. Rev. Lett.* **44** 1285
- [41] Bianco J B and Parodi M 1984 *IEE Conf. on Dielectric Materials, Measurements and Applications (1984)* (London: IEE Publications)
- [42] Boned C and Peyrelasse J 1983 *J. Phys. D: Appl. Phys.* **16** 1777
- [43] Garland J 1966 *Trans. Metall. Soc. AIME* **235** 642
- [44] Sillars R W 1937 *J. Instrum. Electr. Eng.* **80** 378